PHYSICAL REVIEW B **83**, 024511 (2011)

Superconductivity, magnetic order, and quadrupolar order in the filled skutterudite system $Pr_{1-x}Nd_xOs_4Sb_{12}$

P.-C. Ho,[1,2] T. Yanagisawa,[1,*] W. M. Yuhasz,[1,†] A. A. Dooraghi,[1] C. C. Robinson,[1] N. P. Butch,[1,‡] R. E. Baumbach,[1] and M. B. Maple[1]

[1]*Department of Physics, University of California, San Diego, La Jolla, CA 92093-0319, USA*

[2]*Department of Physics, California State University, Fresno, CA 93740-8031, USA*

(Received 3 August 2010; published 31 January 2011)

Superconductivity, magnetic order, and the high field ordered phase have been investigated in the filled skutterudite system $Pr_{1-x}Nd_xOs_4Sb_{12}$ as a function of composition x in magnetic fields up to 9 T and at temperatures between 50 mK and 10 K. Electrical resistivity measurements indicate that the high field ordered phase, which has been identified with antiferroquadruoplar order, persists to $x \sim 0.5$. The superconducting critical temperature T_c of $PrOs_4Sb_{12}$ is depressed linearly with Nd concentration to $x \sim 0.55$, whereas the Curie temperature T_{FM} of $NdOs_4Sb_{12}$ is depressed linearly with Pr composition to $(1-x) \sim 0.45$. In the superconducting region, the upper critical field $H_{c2}(x,0)$ is depressed quadratically with x in the range $0 < x \lesssim 0.3$, exhibits a kink at $x \approx 0.3$, and then decreases linearly with x in the range $0.3 \lesssim x \lesssim 0.6$. The behavior of $H_{c2}(x,0)$ appears to be a result of pair breaking caused by the applied magnetic field and the exchange field associated with the polarization of the Nd magnetic moments in the superconducting state. From magnetic susceptibility measurements, the correlations between the Nd moments in the superconducting state appear to change from ferromagnetic in the range $0.3 \lesssim x \lesssim 0.6$ to antiferromagnetic in the range $0 < x \lesssim 0.3$. Specific-heat measurements on a sample with $x = 0.45$ indicate that magnetic order may occur in the superconducting state, as is also inferred from the depression of $H_{c2}(x,0)$ with x.

DOI: 10.1103/PhysRevB.83.024511 PACS number(s): 74.70.Tx, 65.40.−b, 71.27.+a

I. INTRODUCTION

Since the discovery of heavy-fermion (HF) superconductivity (SC) in $PrOs_4Sb_{12}$ in 2001,[1] this compound has attracted intense interest. It is one of the few Pr compounds that display HF behavior [other examples include $PrInAg_2$ (Ref. 2) and $PrFe_4P_{12}$ (Ref. 3)], it has a high field ordered phase (HFOP) for magnetic fields between 4.5 and 14.5 T and temperatures below 1 K,[4–9] it has been identified with antiferroquadrupolar order,[10] and it exhibits some type of unconventional SC.[11,12] The occurrence of the HFOP can be traced to the small splitting between the ground and first excited states of the Pr^{3+} Hund's rule multiplet by the crystalline electric field (CEF).[11,12] The CEF energy level scheme has been studied in detail, and it is consistent with a nonmagnetic Γ_1 singlet ground state (0 K), a low-lying magnetic $\Gamma_4^{(2)}$ triplet first excited state (∼7 K), a $\Gamma_4^{(1)}$ magnetic triplet excited state (∼130 K), and a nonmagnetic Γ_{23} doublet excited state (∼200 K) in T_h symmetry.[13] Although a Γ_1 ground state does not typically give rise to HF behavior, an intriguing possibility is that the HF state and unconventional SC originate from electric quadrupole fluctuations in the vicinity of a quadrupolar quantum critical point. Various measurements have also provided evidence for multiple SC phases, two-band SC, and point nodes in the SC energy gap.[14–20] Moreover, an internal magnetic field was detected in the SC state by muon spin resonance (μSR) measurements,[21] indicating an unconventional SC state and, possibly, spin-triplet pairing mechanism of electrons.

The end member compound $NdOs_4Sb_{12}$ is a mean-field-type ferromagnet (FM) with a Curie temperature $T_{FM} \approx 1$ K. According to the analysis of magnetic susceptibility, electrical resistivity, and ultrasonic attenuation data, the CEF energy level scheme of the Nd^{3+} ion in $NdOs_4Sb_{12}$ is consistent with a $\Gamma_8^{(2)}$ quartet ground state (0 K), a $\Gamma_8^{(1)}$ quartet first excited state (∼220 K), and a Γ_6 doublet highest excited state (∼590 K), all of which are magnetic in O_h symmetry.[22,23] Recent inelastic neutron-scattering measurements support this energy level scheme with a more accurate description in T_h symmetry: $\Gamma_{67}^{(2)}(0\,\mathrm{K}) - \Gamma_{67}^{(1)}(267\,\mathrm{K}) - \Gamma_5(350\,\mathrm{K})$.[24,25] Although the CEF ground state $\Gamma_{67}^{(2)}$ contains quadrupole moments, no features indicative of a HFOP have been detected in $NdOs_4Sb_{12}$. A large electronic specific-heat coefficient $\gamma \sim 520$ mJ/(mol·K^2) is inferred at low T.[22] In addition to the typical rattling mode that is observed as an ultrasonic dispersion near ∼ 40K in the compounds ROs_4Sb_{12} (R = La, Pr, Nd, and Sm), an extra rattling mode is detected only in $NdOs_4Sb_{12}$.[26] Because the FM transition in $NdOs_4Sb_{12}$ occurs at quite a low T, and the lattice parameter is almost the same as that of $PrOs_4Sb_{12}$, the substitution of Pr with Nd in the pseudoternary system $Pr_{1-x}Nd_xOs_4Sb_{12}$ is well suited to investigating the effect of FM on the evolution of the unconventional SC of $PrOs_4Sb_{12}$.

In this paper, we report the temperature versus Nd concentration $T - x$ phase diagram of the $Pr_{1-x}Nd_xOs_4Sb_{12}$ system. We find that the SC critical temperature T_c of the Pr end member compound decreases linearly with Nd concentration x, while the Curie temperature of the FM end member compound decreases linearly with the Pr concentration $(1-x)$. The SC region extends to $x \approx 0.55$, where it meets the FM phase, with possible evidence for FM ordering of the Nd moments in the SC phase at $x \approx 0.45$. In order to gain information about the evolution of the HFOP with Nd concentration, and to probe the nature of the SC state, magnetoresistive measurements were performed in fields up to 9 T throughout the range $0 \lesssim x \lesssim 0.5$. An analysis of the upper critical field $H_{c2}(x,0)$, involving a comparison to measurements of $H_{c2}(x,0)$ on the $La_{3-x}Gd_xIn$ system and the multiple pair-breaking theory of Fulde and Maki, provides evidence for magnetic ordering of

the Nd ions in the SC state for concentrations above $x \approx 0.3$ and suggests that the SC electrons of $Pr_{1-x}Nd_xOs_4Sb_{12}$ are influenced by magnetic impurities in a manner that is similar to that of the conventional SC La_3In. On the other hand, the evolution of $H_{c2}(x,0)$ might be described in a two-band model of SC. Magnetic susceptibility measurements indicate that the magnetic correlations of the Nd ions change from FM for $0.3 \lesssim x \lesssim 1$ to antiferromagnetic for $0 < x \lesssim 0.3$.

II. EXPERIMENTAL DETAILS

Single crystals of $Pr_{1-x}Nd_xOs_4Sb_{12}$ were grown by the molten flux method as described in Ref. 27. The cubic $LaFe_4P_{12}$-type structure[28] is observed by means of x-ray powder-diffraction measurements throughout the entire doping series. The lattice parameter versus Nd concentration x is plotted in the inset of Fig. 1, where it is apparent that the lattice constant is minimally affected by Nd substitution, consistent with previous measurements by Jeitschko *et al.*[28] The dc magnetic susceptibilities $\chi_{dc}(T)$ (Fig. 1) for collections of single crystals with a total mass near 30 mg were measured using a Quantum Design SQUID magnetometer MPMS-5.5. Together with the x-ray diffraction data, the $\chi_{dc}(T)$ data show that Nd can be substituted continuously for all values of x: i.e., higher values of $\chi_{dc}(T)$ are observed in samples with higher x. The ac magnetic susceptibility $\chi_{ac}(T)$ measurements were performed using home-built first-order gradiometers as pick-up coils in the temperature range from 0.05 to 2.5 K. Each pick-up coil is coupled with a primary coil, which supplies a 17-Hz $\sim 0.05 - 0.15$Oe ac magnetic field. Typically, $\sim 6 - 18$ mg collections of single crystals were used for the $\chi_{ac}(T)$ measurements. Electrical resistivity measurements $\rho(T,H)$ were performed using a standard four-wire technique in a transverse geometry ($H \perp$ current) on individual single crystals mounted in a ^{3}He-^{4}He dilution refrigerator in magnetic fields H between 0 and 9 T. Specific-heat $C(T,H)$ measurements were performed on a collection of single crystals with a mass of 51.07 mg for $x = 0.45$ using a standard heat-pulse technique.

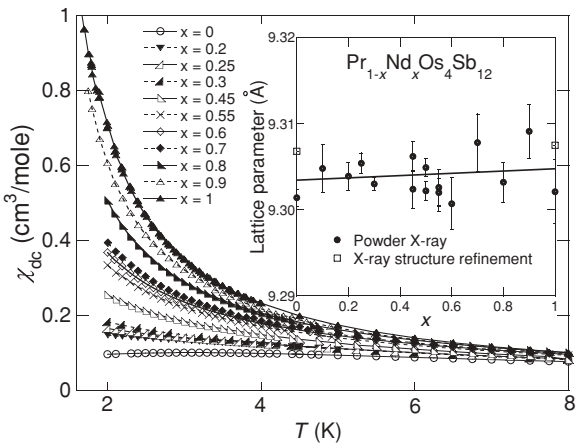

FIG. 1. The dc molar magnetic susceptibility χ_{dc} as a function of temperature T from 2 to 8 K for single crystals of $Pr_{1-x}Nd_xOs_4Sb_{12}$ at various Nd concentrations x. Inset: Nd concentration x dependence of the lattice parameter.

III. RESULTS

The ac magnetic susceptibility data $\chi_{ac}(T)$ for various x are displayed in Fig. 2(a), where the paramagnetic background signal at 2.5 K has been set to zero and the data for each x have been normalized to the largest signal in either the SC or the FM transitions. When a sample enters the SC state, $\chi_{ac}(T)$ drops below the paramagnetic background in a rounded step shape, where the SC transition temperature T_c is defined at 50% of the change in χ_{ac} and the transition width is defined as the difference in the temperatures associated with the 10% and 90% values. When FM ordering occurs, $\chi_{ac}(T)$ exhibits a peak above the paramagnetic background at the FM transition (Curie) temperature T_{FM} and the transition width is taken to be the difference in the temperature corresponding to 90% of the peak value of $\chi_{ac}(T)$ and T_{FM}.

Figure 2(b) summarizes the x dependence of T_c and T_{FM} determined from measurements of $\chi_{ac}(T)$, $\rho(T)$, and $C(T)$. As x increases, the SC transition is suppressed to lower T [at almost the same rate as for $Pr(Os_{1-x}Ru_x)_4Sb_{12}$ (Ref. 29)] and, above $x = 0.6$, only a FM signal appears. For

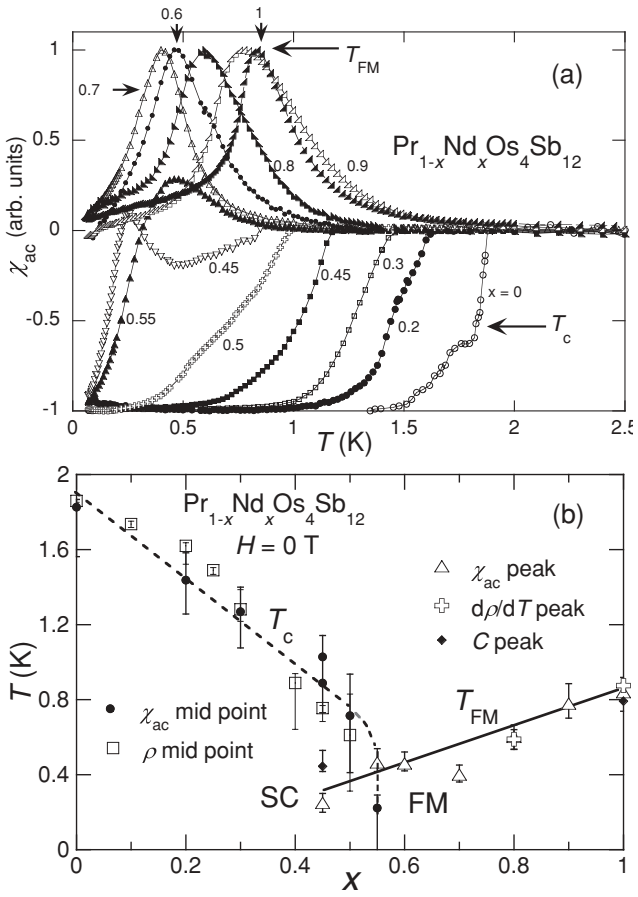

FIG. 2. (a) Temperature T dependence of the ac magnetic susceptibility χ_{ac} in arbitrary units for various Nd concentrations x. (b) SC transition temperature T_c and FM transition (Curie) temperature T_{FM} vs x for $Pr_{1-x}Nd_xOs_4Sb_{12}$ determined from measurements of the ac magnetic susceptibility χ_{ac}, electrical resistivity ρ, and specific heat C. Vertical bars indicate transition widths as defined in the text. For $x = 0.45$, sample "a", which exhibits both SC and FM, T_c is defined as the onset temperature for SC.

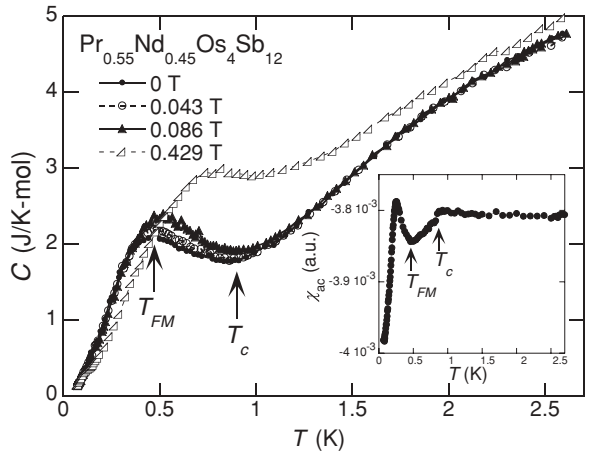

FIG. 3. Specific heat C of $Pr_{0.55}Nd_{0.45}Os_4Sb_{12}$ (batch "a") vs T at $H = 0$, 0.043 , 0.086, and 0.429 T. As H increases, the broad peak moves to higher T. Inset: the corresponding $\chi_{ac}(T)$ measured on single crystals from the same batch.

$x = 0.45 - 0.55$, features associated with both SC and FM are observed. However, we point out the discrepancy between the two $x = 0.45$ samples in Fig. 2(a), which may be caused by supercurrent surface screening in one of the samples that obscures the FM feature in the $\chi_{ac}(T)$ measurements. On the other hand, sample dependence can not be completely ruled out, as these batches were prepared in slightly different ways: For batch "a," the lanthanides were pre-mixed using an arc furnace, prior to being dissolved in the molten metal flux. For batch "b," the lanthanides were not pre-mixed. While batch "a" shows distinct features that are associated with both SC and FM, batch "b" shows a SC transition with a broad tail at low T that might be related to FM. We further note that there is only weak evidence for FM for $x = 0.5$, where a broad hump is observed in $\chi_{ac}(T)$ at low T. From these observations, we infer that the appearance of SC and FM, in this range, is highly sensitive to the growth procedure. However, it does not appear that phase separation is responsible for the differences. We recently performed μSR measurements for $x = 0.45$, 0.5, and 0.55, for which the lanthanides were pre-mixed. For all of these batches, the damping of the μSR signal is described by a single exponential, as expected for a homogeneous system.[30]

The specific heat for specimens from batch "a" where $x = 0.45$ was measured in order to further explore the possible coexistence of SC and FM at this concentration (Fig. 3). A broad peak appears in $C(T, H = 0)$ at 0.9 K with a maximum near 0.48 K. The inset to Fig. 3 shows the corresponding $\chi_{ac}(T)$ data, where the onset of T_c at ~0.9 K matches the beginning of the upturn of the peak in $C(T, H = 0)$. The FM feature then appears in $\chi_{ac}(T)$ near 0.48 K, in agreement with the maximum in $C(T, H = 0)$. These observations support the point of view that FM and SC features are present in both $\chi_{ac}(T)$ and $C(T, H = 0)$ and that the broadness of the peak in $C(T, H = 0)$ may be due to the proximity of the two transitions. Upon application of small magnetic fields, the peak gradually shifts to higher T, indicating that the SC phase is suppressed and the FM phase is enhanced with H. However, since we do not see two distinct peaks, and these measurements were performed on a different set of samples (from batch "a") than were used

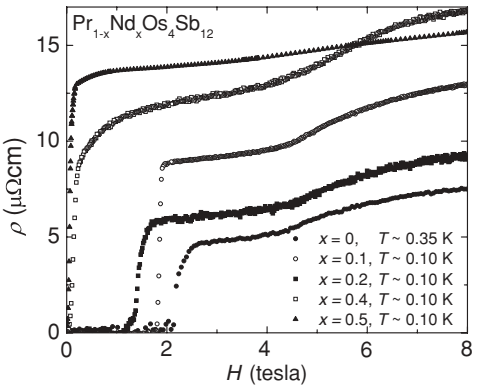

FIG. 4. Electrical resistivity ρ vs magnetic field H at various temperatures T. The rapid drop in $\rho(T, H)$ to zero is due to the SC transition, while the shoulders in $\rho(H)$ above 4 T are due to the HFOP (Ref. 4).

for the ac magnetic susceptibility measurements, these data only provide circumstantial evidence for the coexistence of SC and FM.

From measurements of $\rho(T)$ at constant H and $\rho(H)$ at fixed T (Fig. 4), $H_{c2}(T)$ curves were determined for various values of x (Fig. 5). The data points are defined as the temperatures and fields associated with the 50% value of $\Delta\rho$ at the SC transition, and the transition width is defined as the differences in temperatures and fields corresponding to the 10% and 90% values of $\Delta\rho$ at the SC transition. Above $x = 0.25$, the transition width becomes very large. Measurements of $\rho(H)$ isotherms also reveal the HFOP phase, which appears as a shoulder in $\rho(H)$ above 4 T.[4] The T where the HFOP phase appears is defined as the sharp kink where $\rho(H)$ increases with increasing H.

Since the FM in $NdOs_4Sb_{12}$ conforms to the mean-field model, a Curie-Weiss analysis of the Nd contribution to the magnetic susceptibility should be a good indication of the evolution of FM in the $Pr_{1-x}Nd_xOs_4Sb_{12}$ system. The contribution to the magnetic susceptibility caused by the

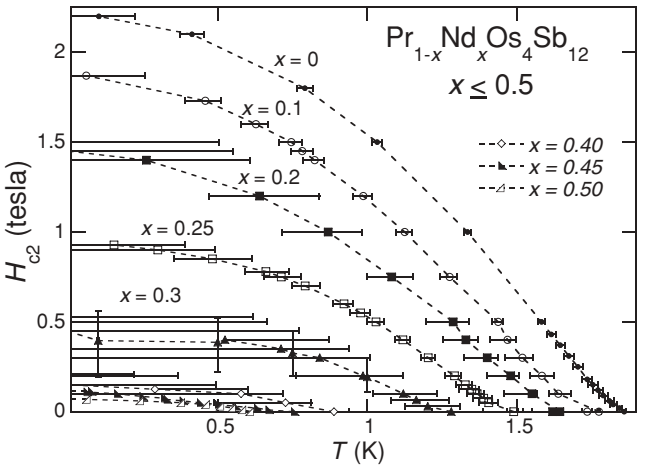

FIG. 5. Temperature dependence of upper critical field H_{c2} for Nd concentrations $x \leqslant 0.5$. The horizontal and vertical bars represent the transition widths, defined from the 10% and 90% values of the drop in $\rho(T, \text{fixed } H)$ at T_c and $\rho(\text{fixed } T, H)$ at H_{c2}.

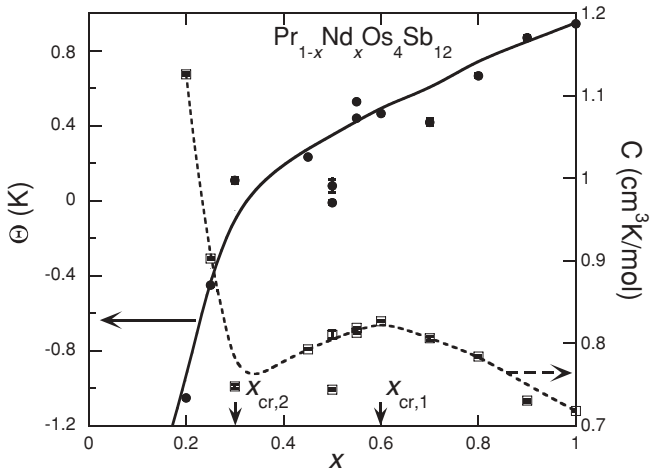

FIG. 6. Nd concentration x dependence of the Curie-Weiss temperature (left axis) Θ and the Curie constant C (right axis) of the Nd^{3+} ion in $Pr_{1-x}Nd_xOs_4Sb_{12}$ after the magnetic susceptibility $\chi_{dc}(T)$ of $PrOs_4Sb_{12}$ has been subtracted. The fitting range is between 2 and 10 K. Solid and dashed lines are guides to the eye.

Pr^{3+} ions is subtracted from $\chi_{dc}(T)$ of $Pr_{1-x}Nd_xOs_4Sb_{12}$ in the following way:

$$\chi_{Nd}(T) = \frac{\chi_{Pr_{1-x}Nd_xOs_4Sb_{12}}(T) - (1-x)\chi_{PrOs_4Sb_{12}}(T)}{x}. \quad (1)$$

We note that, in order to apply this type of analysis, it is necessary to assume that the contribution to $\chi_{dc}(T)$ from the Pr^{3+} ions must retain the same T dependence for all values of x. This seems like a reasonable approximation because the nearest neighbors of the rare-earth ions are Sb ions, which form the cages of the filled skutterudite structure. As such, the CEF that influences each Pr ion is, to first order, unchanged as Pr is replaced with Nd. As a result of the curvature for 20–50 K caused by the effect of the CEF on the Nd^{3+} ions, the Curie-Weiss analysis of $\chi_{Nd}^{-1}(T)$ is only applied in the low-T regime from 2 to 10 K by using the expression

$$\chi_{Nd}(T) = \frac{C}{T-\Theta}, \quad (2)$$

where C is the Curie constant and Θ is the Curie-Weiss (CW) temperature. The fitting results are displayed in Fig. 6. The CW temperature is positive and decreases between $x = 1$ and $x_{cr,2} \sim 0.3$, where it crosses over to a negative value. The Curie constant undergoes a modest increase with decreasing x, with a possible local maximum near $x_{cr1} \sim 0.6$. These results suggest the presence of a weak FM phase between $x \approx 0.3$ and 1 and that antiferromagnetic (AFM) correlations appear below $x \approx 0.3$.

IV. ANALYSIS AND DISCUSSION

Taken together, these results reveal a rich phase diagram for the $Pr_{1-x}Nd_xOs_4Sb_{12}$ system, which includes SC, magnetic order, and quadrupolar order.

Figure 7(a) shows the 0 K $H-x$ phase diagram for $Pr_{1-x}Nd_xOs_4Sb_{12}$. The lower boundary of the high field ordered phase is determined from kinks in the $\rho(H)$ isotherms (Fig. 4). The HFOP in $Pr_{1-x}Nd_xOs_4Sb_{12}$ persists to $x = 0.5$,

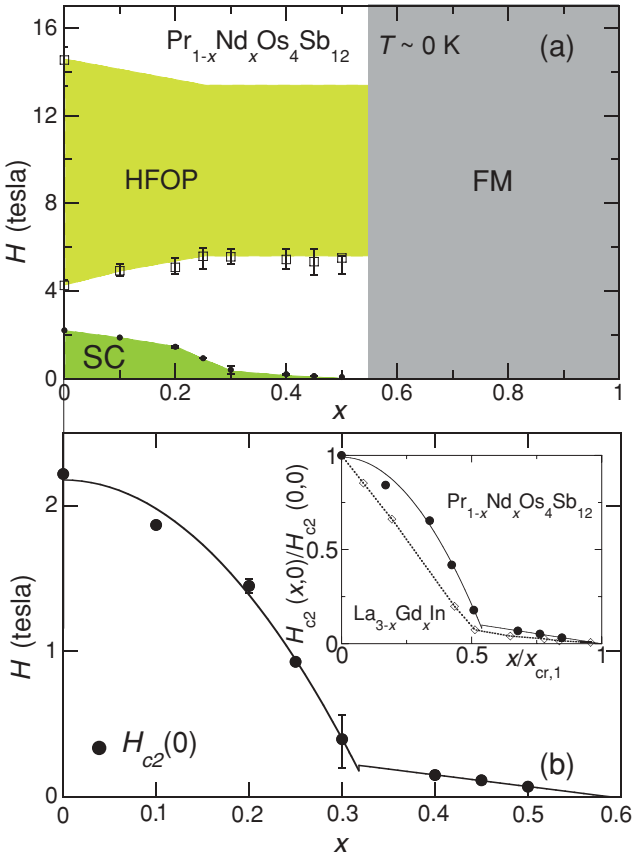

FIG. 7. (Color online) (a) Magnetic field $H-x$ phase diagram of $Pr_{1-x}Nd_xOs_4Sb_{12}$ at ~0 K. (b) Zero-kelvin extrapolation of the experimentally determined upper critical field $H_{c2}(x,0)$. The solid line is a curve based on Eqs. (3). Inset: Normalized $H_{c2}(x,0)$ and x with respect to $H_{c2}(0,0)$ and $x_{cr,1}$ for $Pr_{1-x}Nd_xOs_4Sb_{12}$ and $La_{3-x}Gd_xIn$. Note the difference between the curvature at low concentration.

above which resistivity measurements have not yet been performed, although we note that the features associated with the HFOP are not observed for $NdOs_4Sb_{12}$. The break in slope in the lower $H-x$ phase boundary of the HFOP seems to be correlated with the one observed in $H_{c2}(0)-x$. In addition, the HFOP persists throughout the SC phase in $Pr_{1-x}Nd_xOs_4Sb_{12}$, whereas it vanishes beyond $x \sim 0.1$ in $Pr(Os_{1-x}Ru_x)_4Sb_{12}$.[29] This may be due to changes in the CEF that are larger for Ru substitution for Os than for Nd substitution for Pr.

From the $H_{c2}(x,T)$ data shown in Fig. 5, it can be seen that the magnitude of H_{c2} decreases rapidly with x in the range $0 < x \lesssim 0.3$, more slowly in the range $0.3 \lesssim x \lesssim 0.55$, and appears to vanish near $x \approx 0.6$. This trend is illustrated more clearly in Fig. 7(b), which shows the zero temperature value of the upper critical field $H_{c2}(x,0)$. The $H_{c2}(x,0)$ data can be fit with the equations [solid line in Fig. 7(b)]

$$H_{c2}(x,0) \approx \begin{cases} 2.18 - 19.78x^2 & 0 \leqslant x < 0.3, \\ 0.471 - 0.8x & 0.3 < x < 0.6. \end{cases} \quad (3)$$

where the x dependence of $H_{c2}(0)$ is quadratic for $x \lesssim 0.3$ and is linear for $0.3 \lesssim x \lesssim 0.6$, resulting in an obvious break

in slope near $x \sim 0.3$. Thus, there appear to be two critical concentrations, $x_{cr2} \approx 0.3$ and $x_{cr1} \approx 0.6$. Since evidence for two-band SC has been observed in $PrOs_4Sb_{12}$,[18,19] this result could indicate that Nd substitution has a different effect on the SC of the different bands. If so, then this empirical formula may suggest that one channel has a critical concentration $x_{cr1} \sim 0.6$, for which H_{c2} has a linear x dependence over the entire SC region with a maximum value of ~ 0.471T, while the other channel has a critical concentration $x_{cr2} \sim 0.3$ and only exists in the region $0 \leqslant x \leqslant 0.3$ with a maximum value of $H_{c2} \sim 2.2$T.

In order to explore an alternative route to analyzing the $H_{c2}(x,0)$ data, we turn to the multiple pair-breaking theory of Fulde and Maki.[31–33] For example, this theory has previously been used to analyze the $H_{c2}(x,T)$ curves for the system $La_{3-x}Gd_xIn$, which is formed by substituting Gd impurity ions that carry localized magnetic moments into the singlet BCS SC La_3In.[31] The $H_{c2}(x,0)$ data in the $La_{3-x}Gd_xIn$ system reveal that $H_{c2}(x,0)$ exhibits a rapid linear decrease with x in the lower concentration region and a slower linear depression with x in the higher concentration region. Remarkably, the $H_{c2}(x,0)$ curve for $Pr_{1-x}Nd_xOs_4Sb_{12}$ is quite similar to that of $La_{3-x}Gd_xIn$, as shown in the inset of Fig. 7 where the normalized upper critical field data $H_{c2}(x,0)/H_{c2}(0,0)$ for both systems are plotted versus the normalized concentration x/x_{cr1}. Here, $H_{c2}(0,0)$ is the 0-K H_{c2} of the parent compound without magnetic substituents (i.e., $PrOs_4Sb_{12}$ and La_3In), and $x_{cr,1}$ is the concentration where SC disappears. $H_{c2}(0) \sim 2.25$ T for $PrOs_4Sb_{12}$ and ~ 6.8 T for La_3In, while $x_{cr,1} \sim 0.6$ for $Pr_{1-x}Nd_xOs_4Sb_{12}$ and ~ 0.076 for $La_{3-x}Gd_xIn$. The ratio of $x_{cr,1}$ of $Pr_{1-x}Nd_xOs_4Sb_{12}$ to that of $La_{3-x}Gd_xIn$ is ~ 7.6, or ~ 23 if the magnetic substituent is expressed as the percentage of the overall rare-earth concentration in each compound. For $0 \leqslant x/x_{cr,1} \lesssim 0.5$, the suppression of $H_{c2}(x,0)/H_{c2}(0,0)$ in $Pr_{1-x}Nd_xOs_4Sb_{12}$ is much less than that of $La_{3-x}Gd_xIn$, but for $0.5 \lesssim x/x_{cr,1} \leqslant 1$, both systems have a similar linear monotonic suppression. Interestingly, a break in curvature occurs at $x/x_{cr,1} \sim 0.5$ for both systems. These similarities are surprising, given that the SC state for $PrOs_4Sb_{12}$ is thought to be unconventional.

The generalized Abrikosov-Gorkov (AG) theory of Fulde and Maki includes three effects that can break Cooper pairs in a BCS SC in the presence of magnetic moments and magnetic field: (1) spin polarization of conduction electrons by an applied magnetic field, (2) spin-flip scattering of conduction electrons by magnetic moments, and (3) spin polarization of conduction electrons by the exchange field generated by the applied field or magnetic order mediated by the Ruderman-Kittel-Kasuya-Yosida (RKKY) interaction between the magnetic moments. The generalized AG formula that takes these three effects into account has the following form:

$$\ln\left(\frac{T_c}{T_{c0}}\right) - \Psi\left[\frac{1}{2} - 0.14\left(\frac{T_{c0}}{T_c}\right)\left(\sum_{i=1}^{3}\frac{\alpha_i}{\alpha_{cr,i}}\right)\right] - \Psi\left(\frac{1}{2}\right) = 0, \tag{4}$$

where the SC depairing parameters are denoted as α_i, their critical values as $\alpha_{cr,i}$, and T_{c0} is the SC transition temperature of the parent compound in zero applied magnetic field. Equation (5) describes the total pair-breaking effect in the magnetically substituted SC system, which is equivalent to the pair-breaking effect due only to the applied field on the parent compound:

$$\sum_{i=1}^{3}\frac{\alpha_i}{\alpha_{cr,i}} = \frac{H_{c2}(x,T)}{H_{c2}(0,0)} + \frac{x}{x_{\rm cr}} + \frac{P}{P_{cr}} = \frac{H_{c2}(0,T)}{H_{c2}(0,0)}, \tag{5}$$

where x is the concentration of substituted magnetic ions, $H_{c2}(x,T)$ is the upper critical field for concentration x and temperature T, and P is the Pauli polarization term corresponding to the effect of the magnetic exchange field on the conduction electrons. Following this argument, the temperature dependence of the upper critical field for concentration x can be expressed as

$$H_{c2}(x,T) \approx H_{c2}(0,T) - H_{c2}(0,0)\left(\frac{x}{x_{cr}} + \frac{P}{P_{cr}}\right). \tag{6}$$

The Pauli polarization term $P = \tau_{\rm so}(x\Im\langle J_z\rangle)^2$, where $\tau_{\rm so}$ is the spin-orbit scattering time, $\Im$ is the s-f exchange interaction parameter, and $\langle J_z\rangle$ is the average value of the total angular momentum along the direction of the exchange field, which is defined as the z direction. $\langle J_z\rangle$ has a Brillouin-function dependence on T but approaches a constant value as $T \to 0$ K, which is proportional to the magnetic substituent's "ground-state" magnetic moment. To simplify the analysis, we focus on the behavior at 0 K. In this case, Eqs. (5) and (6) are reduced to

$$H_{c2}(x,0) = H_{c2}(0,0)\left[1 - \left(\frac{x}{x_{cr}} + \frac{\tau_{\rm so}\Im^2 J^2}{P_{cr}}x^2\right)\right]. \tag{7}$$

In the low-concentration regime, $H_{c2}(x,0)$ of $La_{3-x}Gd_xIn$ has a linear x dependence, but $H_{c2}(x,0)$ of $Pr_{1-x}Nd_xOs_4Sb_{12}$ shows a more quadratic behavior. The linear dependence of x in the low-concentration region of $La_{3-x}Gd_xIn$ indicates that the Gd magnetic moments are in the dilute region and no magnetic ordering has developed, so the Pauli polarization contribution is negligible. This suggests that magnetic correlations may be significant in the low-x region for $Pr_{1-x}Nd_xOs_4Sb_{12}$. According to the Curie-Weiss analysis, Θ is negative for $x \lesssim 0.3$, indicating that AFM correlations may be dominant in this concentration range and that the internal magnetic field found in the SC state is associated with AFM order. Thus, the SC in $PrOs_4Sb_{12}$ may be influenced by both AFM and FM correlations that may have comparable strengths over certain parts of the phase diagram. It is possible that the weak suppression of $H_{c2}(0)$ versus x in the range of x from 0 to $x_{cr,2} \approx 0.3$ is due to the combination of pair breaking by the applied field and the AFM exchange field, while the suppression of $H_{c2}(0)$ versus x in the range $x_{cr,2} \approx 0.3$ to $x_{cr,1} \approx 0.6$ could be primarily due to the FM exchange field, although the curvature of $H_{c2}(0)$ in this region is not in agreement with the generalized Abrikosov-Gorkov theory of Fulde and Maki.

V. SUMMARY

The effect of magnetic moments on the normal and SC states of $PrOs_4Sb_{12}$ has been investigated in the $Pr_{1-x}Nd_xOs_4Sb_{12}$ system. In the normal state, the feature associated with the HFOP is clearly observed up to

$x = 0.5$. The kink in the lower phase boundary of the HFOP seems to correlate with a similar feature in $H_{c2}(x,0)$. The HFOP is more robust against substituent concentrations x in $Pr_{1-x}Nd_xOs_4Sb_{12}$ than in the $Pr(Os_{1-x}Ru_x)_4Sb_{12}$ system. The Curie-Weiss analysis for T between 2 and 10 K suggests that FM exists for $0.3 \lesssim x \lesssim 1$ and that AFM correlations are important in the range $x \lesssim 0.3$.

In the SC state, features associated with FM were observed for $x = 0.45 - 0.55$, although more work is needed to verify the coexistence of SC and FM in this region. Quadratic and linear dependences of x were found in $H_{c2}(0)$ for $0 \leqslant x \lesssim 0.3$ and $0.3 \lesssim x \lesssim 0.6$, respectively, which indicates that there are two critical concentrations in the $Pr_{1-x}Nd_xOs_4Sb_{12}$ system: $x_{cr,1} \sim 0.6$ and $x_{cr,2} \sim 0.3$. The break in slope for $H_{c2}(x,0)$ may be related to the existence of two bands of SC electrons in $PrOs_4Sb_{12}$, which are affected by Nd substitution differently. On the other hand, the multiple pair-breaking effect could also explain the behavior in $H_{c2}(x,0)$, where $x_{cr,1}$ and $x_{cr,2}$ are associated with the suppression of SC in the FM and AFM correlation regimes, respectively.

ACKNOWLEDGMENTS

Research at UCSD was supported by the US Department of Energy under Grant No. DE-FG02-04ER46105 for single-crystal growth and characterization and the National Science Foundation under Grant No. DMR 0802478 for low-temperature measurements. Research at California State University, Fresno, was supported by the Research Corporation under the CCSA Grant No. 7669. Research at Hokkaido University was supported by a Grant-in-Aid for Young Scientists (B) from MEXT, Japan.

*Currently at Creative Research Initiative "Sousei," Hokkaido University, Sapporo 001-0021, Japan.
†Currently at Ames Laboratory, Ames, IA 50011, USA.
‡Currently at University of Maryland, USA.

[1] E. D. Bauer, N. A. Frederick, P.-C. Ho, V. S. Zapf, and M. B. Maple, Phys. Rev. B **65**, 100506(R) (2002).
[2] A. Yatskar, W. P. Beyermann, R. Movshovich, and P. C. Canfield, Phys. Rev. Lett. **77**, 3637 (1996).
[3] Y. Aoki, T. Namiki, T. D. Matsuda, K. Abe, H. Sugawara, and H. Sato, Phys. Rev. B **65**, 064446 (2002).
[4] P.-C. Ho, N. A. Frederick, V. S. Zapf, E. D. Bauer, T. D. Do, M. B. Maple, A. D. Christianson, and A. H. Lacerda, Phys. Rev. B **67**, 180508(R) (2003).
[5] R. Vollmer, A. Faisst, C. Pfleiderer, H. v. Löhneysen, E. D. Bauer, P.-C. Ho, V. Zapf, and M. B. Maple, Phys. Rev. Lett. **90**, 057001 (2003).
[6] N. Oeschler, P. Gegenwart, F. Weickert, I. Zerec, P. Thalmeier, F. Steglich, E. D. Bauer, N. A. Frederick, and M. B. Maple, Phys. Rev. B **69**, 235108 (2004).
[7] Y. Aoki, T. Namiki, S. Ohsaki, S. R. Saha, H. Sugawara, and H. Sato, J. Phys. Soc. Jpn. **71**, 2098 (2002).
[8] T. Tayama, T. Sakakibara, H. Sugawara, Y. Aoki, and H. Sato, J. Phys. Soc. Jpn. **72**, 1516 (2003).
[9] C. R. Rotundu, H. Tsujii, Y. Takano, B. Andraka, H. Sugawara, Y. Aoki, and H. Sato, Phys. Rev. Lett. **92**, 037203 (2004).
[10] M. Kohgi *et al.*, J. Phys. Soc. Jpn. **72**, 1002 (2003).
[11] M. B. Maple, N. A. Frederick, P. C. Ho, W. M. Yuhasz, and T. Yanagisawa, J. Supercond. Novel Magn. **19**, 299 (2006).
[12] Y. Aoki, H. Sugawara, H. Harima, and H. Sato, J. Phys. Soc. Jpn. **74**, 209 (2005).
[13] E. A. Goremychkin, R. Osborn, E. D. Bauer, M. B. Maple, N. A. Frederick, W. M. Yuhasz, F. M. Woodward, and J. W. Lynn, Phys. Rev. Lett. **93**, 157003 (2004).
[14] K. Izawa, Y. Nakajima, J. Goryo, Y. Matsuda, S. Osaki, H. Sugawara, H. Sato, P. Thalmeier, and K. Maki, Phys. Rev. Lett. **90**, 117001 (2003).
[15] M.-A. Méasson, D. Braithwaite, G. Lapertot, J.-P. Brison, J. Flouquet, P. Bordet, H. Sugawara, and P. C. Canfield, Phys. Rev. B **77**, 134517 (2008).
[16] M. E. McBriarty, P. Kumar, G. R. Stewart, and B. Andraka, J. Phys. Condens. Matter **21**, 385701 (2009).
[17] K. Grube, S. Drobnik, C. Pfleiderer, H. v. Löhneysen, E. D. Bauer, and M. B. Maple, Phys. Rev. B **73**, 104503 (2006).
[18] M.-A. Méasson, D. Braithwaite, J. Flouquet, G. Seyfarth, J. P. Brison, E. Lhotel, C. Paulsen, H. Sugawara, and H. Sato, Phys. Rev. B **70**, 064516 (2004).
[19] G. Seyfarth, J. P. Brison, M.-A. Measson, J. Flouquet, K. Izawa, Y. Matsuda, H. Sugawara, and H. Sato, Phys. Rev. Lett. **95**, 107004 (2005).
[20] E. E. M. Chia, M. B. Salamon, H. Sugawara, and H. Sato, Phys. Rev. Lett. **91**, 247003 (2003).
[21] Y. Aoki *et al.*, Phys. Rev. Lett. **91**, 067003 (2003).
[22] P.-C. Ho *et al.*, Phys. Rev. B **72**, 094410 (2005).
[23] T. Yanagisawa, W. M. Yuhasz, P.-C. Ho, M. B. Maple, H. Watanabe, T. Ueno, Y. Nemoto, and T. Goto, J. Magn. Magn. Mater. **310**, 223 (2007).
[24] K. Kuwahara, M. Takagi, K. Iwasa, S. Itobe, D. Kikuchi, Y. Aoki, M. Kohgi, H. Sato, and H. Sugawara, Phys. B (Amsterdam) **403**, 903 (2008).
[25] K. Takegahara, H. Harima, and A. Yanase, J. Phys. Soc. Jpn. **70**, 1190 (2001).
[26] T. Yanagisawa, P.-C. Ho, W. M. Yuhasz, M. B. Maple, Y. Yasumoto, H. Watanabe, Y. Nemoto, and T. Goto, J. Phys. Soc. Jpn. **77**, 074607 (2008).
[27] E. D. Bauer, A. Slerbarski, E. J. Freeman, C. Sirvent, and M. B. Maple, J. Phys. Condens. Matter **13**, 4495 (2001).
[28] W. Jeitschko and D. Braun, Acta Crystallogr. Sect. B **33**, 3401 (1977).
[29] P.-C. Ho, N. P. Butch, V. S. Zapf, T. Yanagisawa, N. A. Frederick, S. K. Kim, W. M. Yuhasz, M. B. Maple, J. B. Betts, and A. H. Lacerda, J. Phys. Condens. Matter **20**, 215226 (2008).
[30] P.-C. Ho, L. Shu, S. Zhao, J. M. Mackie, A. A. Dooraghi, T. Yanagisawa, D. E. MacLaughlin, and M. B. Maple (unpublished).
[31] J. E. Crow, R. P. Guertin, and R. D. Parks, Phys. Rev. Lett. **19**, 77 (1967).
[32] P. Fulde and K. Maki, Phys. Lett. **141**, 275 (1966).
[33] M. B. Maple, in *Magnetism: A Treatise on Modern Theory and Materials*, edited by H. Suhl (Academic, New York, 1973), Vol. V, pp. 289–325.